

# Precision Measurement of the Neutral Pion Lifetime

I. Larin,<sup>1,2</sup> Y. Zhang,<sup>3</sup> A. Gasparian\*,<sup>4</sup> L. Gan<sup>†</sup>,<sup>5</sup> R. Miskimen<sup>†</sup>,<sup>2</sup> M. Khandaker<sup>†</sup>,<sup>6</sup> D. Dale<sup>†</sup>,<sup>7</sup>  
S. Danagoulian,<sup>4</sup> E. Pasyuk,<sup>8</sup> H. Gao,<sup>3</sup> A. Ahmidouch,<sup>4</sup> P. Ambrozewicz,<sup>4</sup> V. Baturin,<sup>8</sup> V. Burkert,<sup>8</sup>  
E. Clinton,<sup>2</sup> A. Deur,<sup>8</sup> A. Dolgolenko,<sup>1</sup> D. Dutta,<sup>9</sup> G. Fedotov,<sup>10</sup> J. Feng,<sup>5</sup> S. Gevorkyan,<sup>11</sup> A. Glamazdin,<sup>12</sup>  
L. Guo,<sup>13</sup> E. Isupov,<sup>10</sup> M. M. Ito,<sup>8</sup> F. Klein,<sup>14</sup> S. Kowalski,<sup>15</sup> A. Kubarovskiy,<sup>8</sup> V. Kubarovskiy,<sup>8</sup>  
D. Lawrence,<sup>8</sup> H. Lu,<sup>16</sup> L. Ma,<sup>17</sup> V. Matveev,<sup>1</sup> B. Morrison,<sup>18</sup> A. Micherdzinska,<sup>19</sup> I. Nakagawa,<sup>20</sup> K. Park,<sup>8</sup>  
R. Pedroni,<sup>4</sup> W. Phelps,<sup>21</sup> D. Protopopescu,<sup>22</sup> D. Rimal,<sup>13</sup> D. Romanov,<sup>23</sup> C. Salgado,<sup>6</sup> A. Shahinyan,<sup>24</sup>  
D. Sober,<sup>14</sup> S. Stepanyan,<sup>8</sup> V. V. Tarasov,<sup>1</sup> S. Taylor,<sup>8</sup> A. Vasiliev,<sup>25</sup> M. Wood,<sup>2</sup> L. Ye,<sup>9</sup> and B. Zihlmann<sup>8</sup>  
(PrimEx-II Collaboration)

<sup>1</sup>*Alikhanov Institute for Theoretical and Experimental Physics NRC "Kurchatov Institute", Moscow, 117218, Russia*

<sup>2</sup>*University of Massachusetts, Amherst, MA 01003, USA*

<sup>3</sup>*Duke University and Triangle Universities Nuclear Laboratory, Durham, NC 27708, USA*

<sup>4</sup>*North Carolina A&T State University, Greensboro, NC 27411, USA*

<sup>5</sup>*University of North Carolina Wilmington, Wilmington, NC 28403, USA*

<sup>6</sup>*Norfolk State University, Norfolk, VA 23504, USA*

<sup>7</sup>*Idaho State University, Pocatello, ID 83209, USA*

<sup>8</sup>*Thomas Jefferson National Accelerator Facility, Newport News, VA 23606, USA*

<sup>9</sup>*Mississippi State University, Mississippi State, MS 39762, USA*

<sup>10</sup>*Moscow State University, Moscow 119991, Russia*

<sup>11</sup>*Joint Institute for Nuclear Research, Dubna 141980, Russia*

<sup>12</sup>*Kharkov Institute of Physics and Technology, Kharkov, 310108, Ukraine*

<sup>13</sup>*Florida International University, Miami, FL 33199, USA*

<sup>14</sup>*The Catholic University of America, Washington, DC 20064, USA*

<sup>15</sup>*Massachusetts Institute of Technology, Cambridge, MA 02139, USA*

<sup>16</sup>*Carnegie Mellon University, Pittsburgh, PA 15213, USA*

<sup>17</sup>*School of Nuclear Science and Technology, Lanzhou 730000, China*

<sup>18</sup>*Arizona State University, Tempe, AZ 85281, USA*

<sup>19</sup>*George Washington University, Washington, DC 20064, USA*

<sup>20</sup>*University of Kentucky, Lexington, KY 40506, USA*

<sup>21</sup>*Christopher Newport University, Newport News, VA 23606, USA*

<sup>22</sup>*University of Glasgow, Glasgow G12 8QQ, UK*

<sup>23</sup>*Moscow Engineering Physics Institute, Moscow, Russia*

<sup>24</sup>*Yerevan Physics Institute, Yerevan 0036, Armenia*

<sup>25</sup>*NRC "Kurchatov Institute", Institute for High Energy Physics, Protvino 142281, Russia*

(Dated: February 20, 2020)

The explicit breaking of the axial symmetry by quantum fluctuations gives rise to the so-called axial anomaly. This phenomenon is solely responsible for the decay of the neutral pion  $\pi^0$  into two photons, leading to its unusually short lifetime. We measured the decay width  $\Gamma$  of the  $\pi^0 \rightarrow \gamma\gamma$  process with unprecedented precision. The differential cross sections for  $\pi^0$  photoproduction at forward angles were measured on two targets:  $^{12}\text{C}$  and  $^{28}\text{Si}$ , yielding  $\Gamma(\pi^0 \rightarrow \gamma\gamma) = 7.798 \pm 0.056$  (stat.)  $\pm 0.109$  (syst.) eV. Combining the results of this and an earlier experiment led to a weighted average of  $\Gamma(\pi^0 \rightarrow \gamma\gamma) = 7.802 \pm 0.052$  (stat.)  $\pm 0.105$  (syst.) eV. Our final result has a total uncertainty of 1.50% and confirms the prediction based on the chiral anomaly in quantum chromodynamics.

PACS numbers: 11.80.La, 13.60.Le, 25.20.Lj

The basic symmetries of the classical world are at the origin of the most fundamental conservation laws. Classical symmetries are generally respected in the quantum realm, but it was realized several decades ago that there are exceptions to this rule in the form of so-called "anomalies". The most famous one is arguably the axial anomaly, which enables a process of decay of a light hadron called the neutral  $\pi$  meson into two photons, denoted as  $\pi^0 \rightarrow \gamma\gamma$ .  $\pi$  mesons were first proposed by Yukawa [1] as the intermediaries of nuclear interactions; they result from a profound phenomenon central to strong interaction physics described by Quantum

Chromodynamics (QCD), the theory of quarks and gluons. These three pions ( $\pi^+$ ,  $\pi^-$  and  $\pi^0$ ) consist of light quark-antiquark pairs coupled together by exchange of gluons. The axial anomaly is represented by truly unique graphs in perturbative quantum field theory that do not require renormalization, thereby enabling a purely analytical prediction from QCD – the  $\pi^0$  lifetime. Generally, QCD can analytically predict only relative features and needs either experimental data, models or numerical inputs on the lattice, to anchor these relative predictions. Thus, experimental verification of this phenomenon with highest accuracy is a unique test of quantum field theory

\*spokesperson, corresponding author, gasparian@jlab.org

†spokesperson

and of symmetry breaking by pure quantum effects [2].  
 The fact that the three light quarks,  $u$ ,  $d$  and  $s$ , have much smaller masses than the energy scale of QCD gives rise to an approximate chiral flavor symmetry consisting of chiral left-right and axial symmetries. The chiral symmetry is spontaneously broken by the non-perturbative dynamics of QCD which leads to the condensation of quark pairs, the  $\langle\bar{q}q\rangle$  condensate. This phenomenon is responsible for the observed octet of light pseudoscalar mesons in nature, with  $\pi^0$  being one of them. The axial symmetry is explicitly broken by the quantum phenomenon known as the axial (or chiral) anomaly [3], originating from the quantum fluctuations of the quark and gluon fields. The chiral anomaly drives the decay of the  $\pi^0$  into two photons with the predicted decay width [4]:

$$\Gamma(\pi^0 \rightarrow \gamma\gamma) = \frac{m_{\pi^0}^3 \alpha^2 N_c^2}{576\pi^3 F_{\pi^0}^2} = 7.750 \pm 0.016 \text{ eV},$$

where  $\alpha$  is the fine-structure constant,  $m_{\pi^0}$  is the mass,  $N_c = 3$  is the number of colors in QCD, and  $F_{\pi^0}$  is the pion decay constant;  $F_{\pi^0} = 92.277 \pm 0.095 \text{ MeV}$  extracted from the charged pion weak decay [5]; note that there are no free parameters.

The study of corrections to the chiral anomaly prediction has been mainly done with Chiral Perturbation Theory (ChPT), with the three light flavors. The dominant corrections are the result of meson state mixing caused by the differences between the quark masses. The  $\pi^0$  mixes with the  $\eta$  and  $\eta'$  meson owing to the isospin symmetry breaking, which is in turn a consequence of  $m_u < m_d$ ; the correction is calculable in a global analysis of the three neutral mesons [6]. In ref. [6] the  $\Gamma(\pi^0 \rightarrow \gamma\gamma)$  width was calculated in a combined framework of ChPT and  $1/N_C$  expansion up to  $\mathcal{O}(p^6)$  and  $\mathcal{O}(p^4 \times 1/N_C)$  in the decay amplitude (GBH, NLO). Their result,  $\Gamma(\pi^0 \rightarrow \gamma\gamma) = 8.10 \pm 0.08 \text{ eV}$  with  $\sim 1\%$  estimated uncertainty is about 4.5% higher than the prediction of chiral anomaly. Another Next-to-Leading-Order (NLO) calculation in ChPT was performed in [7], resulting in  $8.06 \pm 0.06 \text{ eV}$  (AM, NLO). The only Next-to-Next-to-Leading-Order (NNLO) calculation for the decay width was performed in [8] yielding a similar result,  $8.09 \pm 0.11 \text{ eV}$ . The calculations of the corrections to the chiral anomaly in the framework of QCD using dispersion relations and sum rules in ref. [9] resulted in the value of  $7.93 \pm 0.12 \text{ eV}$ , which is about 2% lower than the ChPT predictions. The fact that these calculations performed by different methods differ from the chiral anomaly prediction by a few percent, with an accuracy of approximately one percent, makes the precision measurement of the  $\pi^0 \rightarrow \gamma\gamma$  width a definitive low-energy test of QCD.

In past decades, there have been extensive efforts to measure the  $\pi^0$  radiative decay width using three experimental methods: the Primakoff, the direct, and the collider methods. The current Particle Data Group (PDG) value of  $\pi^0 \rightarrow \gamma\gamma$  decay width is  $7.63 \pm 0.16 \text{ eV}$  [5]. It is the average of five

measurements: two Primakoff type, Cornell University (Cornell, (Prim.)) [10] with  $7.92 \pm 0.42 \text{ eV}$ , and Jefferson Laboratory (JLab, PrimEx-I (Prim.)) [11] with  $7.82 \pm 0.14 \text{ (stat.)} \pm 0.17 \text{ (syst.) eV}$ ; a direct measurement, European Center for Nuclear Research (CERN (Dir.)) [12] with  $7.25 \pm 0.18 \text{ (stat.)} \pm 0.14 \text{ (syst.) eV}$ ; a collider measurement by Crystal Ball (CBAL (Col.)) at Deutsches Electronen-Synchrotron (DESY) [13] with  $7.7 \pm 0.72 \text{ eV}$ ; a measurement from radiative PIon BETA decay (PIBETA) [14] with  $7.74 \pm 1.02 \text{ eV}$ . The result from the PrimEx-I experiment [11] improved the uncertainty on the decay width quoted in the previous PDG [15] value by a factor of two-and-a-half and confirmed the validity of the chiral anomaly at the few percent level. However, there is a 6% discrepancy between the two most precise experiments included in the PDG average, the CERN direct [12] and PrimEx-I Primakoff [11]. Furthermore, the accuracy of the PDG average is still not adequate to test the theory corrections to the prediction of the anomaly. The PrimEx-II experiment was conducted at JLab to address these issues.

To reach a percent level precision in the extracted  $\pi^0 \rightarrow \gamma\gamma$  decay width we have implemented several basic improvements in the experimental technique (schematically shown in Fig. 1) used in the previous Primakoff type of experiments. The existing tagged photon beam facility (Tagger [16]) in Hall B at JLab was used allowing critical improvements in the background separation and the determination of the photon flux. Instead of the traditionally used Pb-glass based electromagnetic calorimeter, used in the previous experiments, we developed and constructed a novel PbWO<sub>4</sub> crystal based multi-channel, high resolution and large acceptance electromagnetic calorimeter (HyCal) [17]. The combination of these two techniques greatly improved the angular resolution of the photoproduced  $\pi^0$ s, which is critical for Primakoff type measurements, and significantly reduced the systematic uncertainties that were present in previous experiments. In addition, the cross sections of two well-known electromagnetic processes, Compton scattering and  $e^+e^-$  pair production from the same experimental target, were periodically measured during the experiment to validate the extracted  $\pi^0$  photoproduction cross sections and their estimated systematic uncertainties. Tagged photons with known energy and timing were incident on the production targets located in the entrance of the large acceptance dipole magnet (8% radiation length (r.l.) <sup>12</sup>C and 10% r.l. <sup>28</sup>Si solid targets were used). This magnet played two important roles in the experiment: deflect all charge particles produced in the target from the HyCal acceptance; and detection of  $e^+e^-$  pairs produced in the target (Pair Spectrometer, PS) allowing continuous measurement of the relative photon tagging efficiencies during the experiment. The decay photons from the photoproduced  $\pi^0$ s traveled through the Vacuum Chamber (VCh) and the Helium Bag (HB) and were detected in the HyCal calorimeter located 7 m

downstream from the targets. Two-planes of scintillator counters (Veto Counters, VC), located in front of HyCal, provided rejection of charged particles and effectively reduced the background in the experiment. A more detailed description of the experimental setup is presented in the Supplementary Materials (section S2). In this experiment we measured the differential cross sections for the photoproduced  $\pi^0$  mesons at forward angles on two targets. At these small angles the  $\pi^0$ 's are produced by two different elementary mechanisms: by one photon exchange (the so-called Primakoff process) and by a hadron exchange (the so-called strong process). The amplitudes of these processes contribute both coherently and incoherently in the  $\pi^0$  photoproduction cross sections at forward angles (see Eq. S1). The cross section of the Primakoff process is directly proportional to the  $\pi^0 \rightarrow \gamma\gamma$  decay width, allowing its extraction from the measured differential cross sections with high accuracy. More detail description of these processes and our fitting procedure to extract the decay width is presented in Section S3.

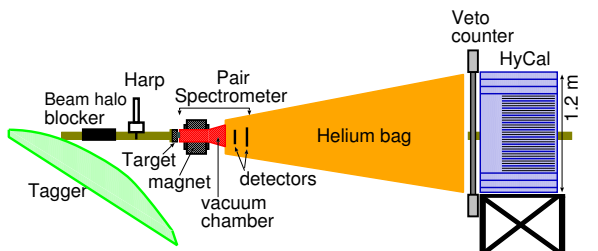


FIG. 1: Schematic view of the PrimEx-II experimental setup (not to scale, see the text for description of individual detectors and components).

PrimEx-I achieved a total uncertainty of 2.8% in the extracted width  $\Gamma(\pi^0 \rightarrow \gamma\gamma)$  [11]. The PrimEx-II experiment aimed to significantly increase the statistics and improve the systematic uncertainties to reach the percent level accuracy. The following was implemented to increase the statistics by a factor of six: (i) the accepted energy interval of the tagged photons was increased by 50%; (ii) thicker solid targets were used: 8% radiation length (r.l.)  $^{12}\text{C}$  and 10% r.l.  $^{28}\text{Si}$ ; (iii) the performance of the data acquisition (both at electronics and software levels) was upgraded to increase the data taking rate by a factor of five. The systematic uncertainties were also reduced thanks to several improvements: (i) the central part of the HyCal (about 400 modules) was equipped with individual Time-to-Digital Converters (TDC) for better rejection of time accidental events; (ii) the trigger for the experiment was simplified by using only events with a total deposited energy above 2.5 GeV in HyCal; (iii) a new set of 12 horizontal scintillator veto counters was added for better rejection of charged particles in HyCal (see Fig. 1); (iv) the distance between the calorimeter and target was reduced to 7 m, which al-

lowed for better geometrical acceptance between  $1.0^\circ$  to  $2.0^\circ$  in the  $\pi^0$  production angles, and improved separation of the nuclear coherent and incoherent production terms from the Primakoff process in the measured cross sections (see Eq. S1). In addition, the improved running conditions (beam intensity and position stability, etc.) of the JLab accelerator allowed for a significant reduction of the beam-related systematic uncertainties. Using an intermediate-atomic-number target,  $^{28}\text{Si}$ , in combination with a low-atomic-number target,  $^{12}\text{C}$ , allowed more effective control of systematic uncertainties related to the extraction of the Primakoff contribution. Similar to the PrimEx-I experiment [11], the combination of the photon tagger with its well-defined photon energy and timing together with the HyCal calorimeter defined the event selection criteria.

The event yield (the number of elastically produced  $\pi^0$  events for each angular bin) was extracted using the kinematic constraints and by fitting the experimental two-photon invariant mass spectra ( $M_{\gamma\gamma}$ ) to subtract the background contributions. Two independent analysis methods, the “constrained” and “hybrid” mass methods were used to extract the event yield in this experiment. The two methods (integrated over the angular range of  $\theta_\pi = 0^\circ$ – $2.5^\circ$  and for the incident energies  $E_\gamma = 4.45$ – $5.30$  GeV) agree with each other. The total integrated statistics was about 83,000  $\pi^0$  events on  $^{12}\text{C}$  and 166,000 on  $^{28}\text{Si}$  targets, a factor of six increase compared to PrimEx-I. This reduced the statistically limited part of the systematic uncertainties in the yield extraction process. Combining the two analysis methods with the partially independent systematics further reduced the systematic uncertainty to 0.80%. This includes the uncertainty in the physics background subtraction, 0.10%, mostly from  $\omega$  mesons photoproduction. High precision monitoring of the photon beam flux during the entire data taking process is one of the challenging tasks for this type of experiment [18]. The photon tagger was used for measurements of the photon beam flux, a Total Absorption Counter (TAC) for periodic measurements of the absolute tagging ratios, and a pair-spectrometer (PS) for continuous monitoring of the relative tagging ratios and tagger stability [18]. The stability of the beam parameters (position, width, and frequency of interruptions) was far better than during PrimEx-I. That, and more frequent TAC measurements, led to a better measurement of the photon flux (0.80% relative uncertainty was reached in this experiment). Different measurement methods allowed to achieve a sub-percent accuracy for the uncertainty in the number of target nuclei per  $\text{cm}^2$ : less than 0.10% for  $^{12}\text{C}$  and 0.35% for  $^{28}\text{Si}$  targets [19, 20]. The geometrical acceptances and resolutions of the experimental setup have been calculated by a standard nuclear physics Monte Carlo simulation package. The contributed uncertainty in the extracted cross sections from this part is estimated to be 0.55%.

The extracted differential cross sections of  $\pi^0$  photo-

258 production on both  $^{12}\text{C}$  and  $^{28}\text{Si}$  are shown in Fig. 2.  
 259 They are integrated over the incident photon beam en-  
 260 ergies of 4.45 to 5.30 GeV (with the weighted average  
 261 value of 4.90 GeV). The fit results for the four processes  
 262 contributing to forward production: Primakoff, nuclear  
 263 coherent, interference between them, and nuclear inco-  
 264 herent are also shown.

265 The  $\pi^0 \rightarrow \gamma\gamma$  decay width was extracted by fitting the  
 266 experimental differential cross sections to the theoretical  
 267 terms of four contributing processes (see Eq. S1), con-  
 268 voluted with the angular resolution, experimental accep-  
 269 tances and folded with the measured incident incident photon en-

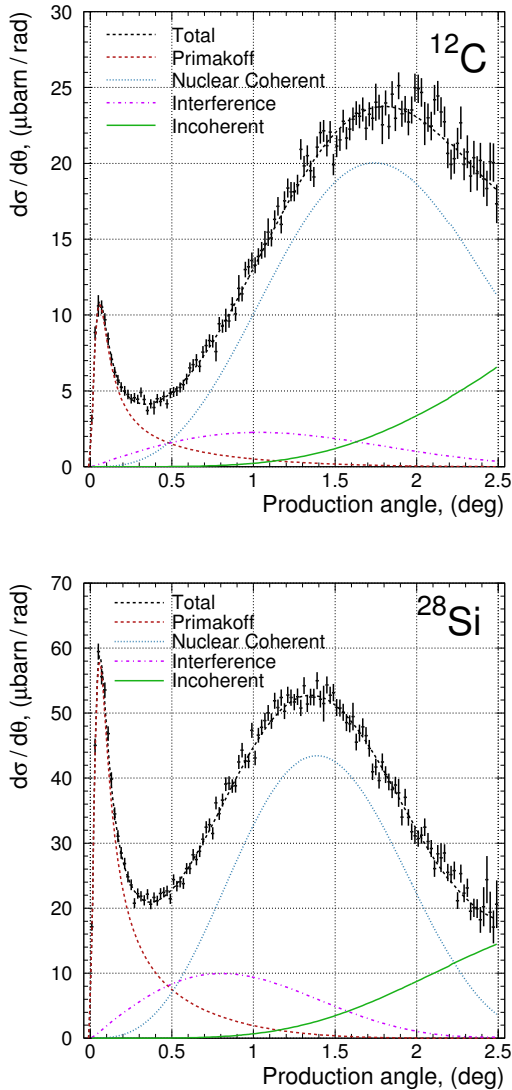


FIG. 2: Experimental differential cross section as a function<sup>290</sup>  
 of the  $\pi^0$  production angle for  $^{12}\text{C}$  (top) and  $^{28}\text{Si}$  (bottom)<sup>291</sup>  
 together with the fit results for the different physics processes<sup>292</sup>  
 (see insert and text for explanations).<sup>293</sup>

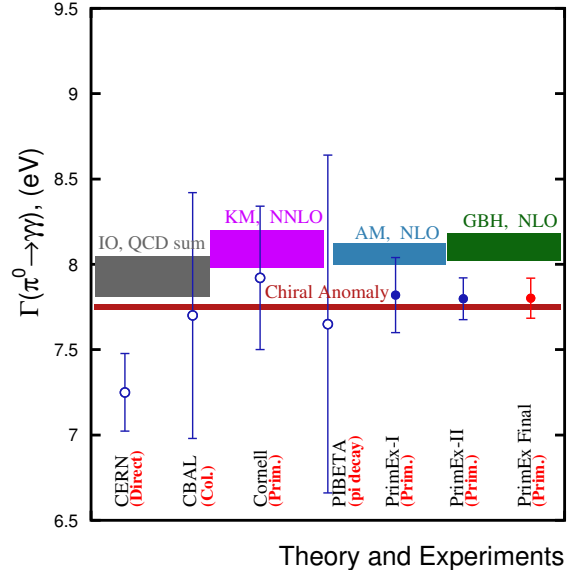


FIG. 3: Theoretical predictions and experimental results of the  $\pi^0 \rightarrow \gamma\gamma$  decay width. Theory: chiral anomaly [3] (dark red band); IO, QCD sum rule [9] (gray band); KM, ChPT NNLO [8] (magenta band); AM, ChPT NLO [7] (blue band); GBH, ChPT NLO [6] (green band). Experiments included in the current PDG [5]: CERN direct [12]; Crystal Ball collider [13]; Cornell Primakoff [10]; PIBETA [14]; PrimEx-I [11]. Our new results: PrimEx-II and the PrimEx combined.

270 ergy spectrum. The effect of final state interactions be-  
 271 tween the outgoing pion and the nuclear target, and the  
 272 photon shadowing effect in nuclear matter must be ac-  
 273 curately included in the theoretical cross sections for the  
 274 precise extraction of the Primakoff term, and therefore,  
 275  $\Gamma(\pi^0 \rightarrow \gamma\gamma)$  [21, 22]. Within our collaboration, two sep-  
 276 arate groups analyzed the data using different methods.  
 277 They extracted  $\Gamma(\pi^0 \rightarrow \gamma\gamma)$  from their cross sections us-  
 278 ing similar fitting procedures (shown in Table S1). Thus,  
 279 for the same target, the statistical and part of the system-  
 280 atic uncertainties from the two analysis groups are cor-  
 281 related. This was accounted for when the two results were  
 282 combined [23]. Results for the individual targets were  
 283 obtained by using the weighted average method, yield-  
 284 ing:  $\Gamma(\pi^0 \rightarrow \gamma\gamma) = 7.763 \pm 0.127 \text{ (stat.)} \pm 0.117 \text{ (syst.)} \text{ eV}$   
 285 for  $^{12}\text{C}$ , and  $7.806 \pm 0.062 \text{ (stat.)} \pm 0.109 \text{ (syst.)} \text{ eV}$  for  
 286  $^{28}\text{Si}$ . The results from the two different targets were  
 287 then combined to give the final result:  $\Gamma(\pi^0 \rightarrow \gamma\gamma) =$   
 288  $7.798 \pm 0.056 \text{ (stat.)} \pm 0.109 \text{ (syst.)} \text{ eV}$ , with a total un-  
 289 certainty of 1.57% (see Fig. 3).

290 To check the sensitivity of the extracted decay width to  
 291 the theory parameters (nuclear matter density, nuclear  
 292 radii, photon shadowing parameter,  $\pi^0 N$  total cross sec-  
 293 tion, etc.), the values of these parameters were changed  
 294 by several sigmas and the cross sections were refitted to

295 obtain new decay widths. Using this procedure, the two<sub>352</sub>  
 296 main contributors to the systematic uncertainties were<sub>353</sub>  
 297 found to be the nuclear radii and the photon shadowing<sub>354</sub>  
 298 parameter ([24], [25]). The nuclear coherent process,<sub>355</sub>  
 299 which dominates at larger angles for both targets,<sub>356</sub>  
 300 was determined with a high precision (see Fig. 2), and<sub>357</sub>  
 301 this information was used to extract the nuclear radii<sub>358</sub>  
 302 for the targets. To do so, the radii were varied around<sub>359</sub>  
 303 the experimental values obtained from electron scatter-<sub>360</sub>  
 304 ing data [26, 27], known to better than 0.6%. Then, the<sub>361</sub>  
 305 best values for the nuclear radii were defined by min-<sub>362</sub>  
 306 imizing the resulting  $\chi^2$  distributions. Our extracted<sub>363</sub>  
 307 results for the nuclear radii are:  $2.457 \pm 0.047$  fm for<sub>364</sub>  
 308  $^{12}\text{C}$  and  $3.073 \pm 0.018$  fm for  $^{28}\text{Si}$ . They agree with the<sub>365</sub>  
 309 radii extracted from electron scattering [26, 27]. The<sub>366</sub>  
 310 shadowing parameter was extracted by a similar proce-<sub>367</sub>  
 311 dure. The extracted value is:  $\xi = 0.30 \pm 0.17$ , agreeing<sub>368</sub>  
 312 with two previous measurements: 0.25–0.50 from [24] and<sub>369</sub>  
 313  $0.31 \pm 0.12$  from [25]. Varying this parameter within a  $3\sigma$ <sub>370</sub>  
 314 interval gave only a 0.30% uncertainty in the extracted<sub>371</sub>  
 315  $\Gamma(\pi^0 \rightarrow \gamma\gamma)$  (correlated between the two targets). Our<sub>372</sub>  
 316 systematic uncertainties are described in greater detail<sub>373</sub>  
 317 in Section S3 and are summarized in Tables S2 and S3.<sub>374</sub>

318 For both PrimEx-I and PrimEx-II, the experimental<sub>375</sub>  
 319 uncertainties have been validated by periodically measur-<sub>376</sub>  
 320 ing the Compton cross sections for the same nuclear tar-<sub>377</sub>  
 321 gets. Our measured Compton cross sections agree with<sub>378</sub>  
 322 the theoretical simulations of this well-known Quantum<sub>379</sub>  
 323 Electrodynamics (QED) process to better than 1.7% [28].<sub>380</sub>

324 If the results from the two PrimEx experiments<sub>381</sub>  
 325 are combined, correlations between different sys-<sub>382</sub>  
 326 tematic uncertainties can be accounted for [23].<sub>383</sub>  
 327 The weighted average final result for the  $\pi^0 \rightarrow$ <sub>384</sub>  
 328  $\gamma\gamma$  decay width from the two PrimEx experi-<sub>385</sub>  
 329 ments is  $7.802 \pm 0.052$  (stat.)  $\pm 0.105$  (syst.) eV (shown<sub>386</sub>  
 330 in Fig. 3), defining the new lifetime:  $\tau = 8.337 \pm$ <sub>387</sub>  
 331  $0.056$  (stat.)  $\pm 0.112$  (syst.)  $\times 10^{-17}$  s. With 1.50% to-<sub>388</sub>  
 332 tal uncertainty, this is the most precise measurement of<sub>389</sub>  
 333 the  $\Gamma(\pi^0 \rightarrow \gamma\gamma)$ , and firmly confirms the prediction<sub>390</sub>  
 334 of the chiral anomaly in QCD at the percent level. As seen<sub>391</sub>  
 335 from Fig. 3, our result deviates from the theoretical cor-<sub>392</sub>  
 336 rections to the anomaly by two standard deviations.<sub>393</sub>

337 The axial anomaly, which has historically provided<sub>394</sub>  
 338 strong evidence in favor of the color-charge concept in<sub>395</sub>  
 339 QCD, continues to teach us about the most fundamental<sub>396</sub>  
 340 aspects of nature, for example, by strictly constraining<sub>397</sub>  
 341 physics beyond the Standard Model (SM) and present-<sub>398</sub>  
 342 ing a unique opportunity for measuring the light quark<sub>399</sub>  
 343 mass ratio. The  $\Gamma(\pi^0 \rightarrow \gamma\gamma)$  decay width is a critical in-<sub>400</sub>  
 344 put for the normalization of the  $\pi^0$  transition form factor<sub>401</sub>  
 345 to constrain the hadronic light-by-light scattering contri-<sub>402</sub>  
 346 butions to the well-known muon (g-2) anomaly in search<sub>403</sub>  
 347 of new physics [29]. The light quark masses are as yet un-<sub>404</sub>  
 348 measured, and whether the masses are in fact observable<sub>405</sub>  
 349 is still under debate. Future directions include measur-<sub>406</sub>  
 350 ing the anomaly driven  $\eta \rightarrow \gamma\gamma$  decay, which provides<sub>407</sub>  
 351 unique normalization to the isospin-violating  $\eta \rightarrow 3\pi$  de-<sub>408</sub>  
 352

353 cay that leads to a model independent extraction of the  
 354 light quark mass ratio [30].

---

- [1] H. Yukawa Proc. Math. Soc. Jpn. **17**, 48 (1935).
- [2] S. Weinberg, “The quantum theory of fields”, Cambridge University Press. (1996), v.2
- [3] J. S. Bell and R. Jackiw, Nuovo Cimento A **60**, 47 (1969); S. L. Adler, Phys. Rev. **177**, 2426 (1969).
- [4] A. M. Bernstein and B. R. Holstein, Rev. Mod. Phys. **85**, 49 (2013).
- [5] M. Tanabashi *et al.*, Phys. Rev. D **98**, 030001 (2018).
- [6] J. L. Goity, A. M. Bernstein, B. R. Holstein, Phys. Rev. D **66**, 076014 (2002).
- [7] B. Ananthanarayan and B. Moussallam, JHEP **0205**, 052 (2002).
- [8] K. Kampf and B. Moussallam, Phys. Rev. D **79**, 076005 (2009).
- [9] B. L. Ioffe and A. G. Oganesian, Phys. Lett. B **647**, 389 (2007).
- [10] A. Bowman *et al.*, Phys. Rev. Lett. **33**, 1400 (1974).
- [11] I. Larin *et al.*, Phys. Rev. Lett. **106**, 162303 (2011).
- [12] H. W. Atherton *et al.*, Phys. Lett. **B158**, 81 (1985).
- [13] D. Williams *et al.*, Phys. Rev., D38:1365, 1988.
- [14] M. Bychkov *et al.*, Phys. Rev. Lett. **103**, 051802 (2009).
- [15] C. Amsler *et al.* (Particle Data Group), Physics Letters B667, 1 (2008).
- [16] D. I. Sober *et al.*, Nucl. Instrum. and Methods A **440**, 263 (2000).
- [17] A. Gasparian Proc. XI Int. Conf. Calorim. Part. Phys. **1**, 109 (2004).
- [18] A. Teymurazyan *et al.*, Nucl. Instrum. and Methods A **767**, 300 (2014).
- [19] P. Martel *et al.*, Nucl. Instr. and Meth.A **612**, 46 (2009).
- [20] C. Harris, R. Miskimen [http://www.jlab.org/primex/primex\\_notes/SiTarget.pdf](http://www.jlab.org/primex/primex_notes/SiTarget.pdf).
- [21] S. Gevorkyan *et al.*, Phys. Rev. **C80**, 055201 (2009).
- [22] S. Gevorkyan, *et al.*, Phys. Part. Nucl. Lett. **9**, 3 (2012).
- [23] I. Larin, PrimEx technical notes ([https://www.jlab.org/primex/primex\\_notes/PrimEx\\_II\\_uncert.pdf](https://www.jlab.org/primex/primex_notes/PrimEx_II_uncert.pdf)).
- [24] W. T. Meyer *et al.*, Phys. Rev. Lett., **28**, 1344 (1972).
- [25] A. Boyarski *et al.*, Phys. Rev. Lett., **23**, 1343 (1969).
- [26] H. De Vries, C. W. De Jager and C. De Vries, At. Data Nucl. Data Tables **36**, 495 (1987).
- [27] E. A. J. M. Offermann *et al.*, Phys. Rev. C **44**, 1096 (1991).
- [28] P. Ambrozewicz *et al.*, Phys. Lett. B, **797**, 134884 (2019).
- [29] M. Hoferichter *et al.*, Phys. Rev. Lett., **121**, 112002 (2018).
- [30] A. Gasparian *et al.*, JLab Proposal E12-10-011. ([http://www.jlab.org/exp\\_prog/proposals/10/PR12-10-011.pdf](http://www.jlab.org/exp_prog/proposals/10/PR12-10-011.pdf)).
- [31] H. Primakoff, Phys. Rev., **81**, 899 (1951).
- [32] I. Larin, PrimEx technical notes ([https://www.jlab.org/primex/primex\\_notes/tac.pdf](https://www.jlab.org/primex/primex_notes/tac.pdf)).
- [33] T. E. Rodrigues, PrimEx technical notes ([https://www.jlab.org/primex/primex\\_notes/PrimEx\\_Note\\_52.pdf](https://www.jlab.org/primex/primex_notes/PrimEx_Note_52.pdf)).

**Acknowledgments:** We are grateful to the Accelerator and Physics Divisions at Jefferson Lab which made these experiments possible. We thank the Hall B engi-

412 neering and physics staff for their critical contributions  
413 during all stages of these experiments. Theoretical sup-  
414 port provided by Jose Goity throughout this project is  
415 gratefully acknowledged. This project was supported in  
416 part by the National Science Foundation under a Major  
417 Research Instrumentation grant (PHY-0079840) and by  
418 the U.S. Department of Energy, including contract No.  
419 DE-AC05-06OR23177 under which the Jefferson Science<sub>451</sub>  
420 Associates, LLC operates Thomas Jefferson National  
421 Accelerator Facility.

422

423

424